QUANTITATIVE MAGNETIC RESONANCE IMAGING OF BRAIN DEVELOPMENT IN PREMATURE AND MATURE NEWBORNS

Petra S. Hüppi M.D.[1], Simon Warfield Ph.D.[2], Ron Kikinis M.D.[2],Patrick D. Barnes M.D.[3], Gary P. Zientara Ph.D.[2], Ferenc A. Jolesz M.D.[2], Miles K. Tsuji, M.D.[1], and Joseph J. Volpe M.D.[3]

[1] Joint Program in Neonatology, Harvard Medical School, Boston

[2] Department of Radiology and MRI Division, Brigham and Women's Hospital, Harvard Medical School, Boston

[3] Department of Radiology, Children's Hospital, Harvard Medical School, Boston , Department of Neurology, Children's Hospital, Harvard Medical School, Boston

Petra S Hüppi, MD

Joint Program in Neonatology, Harvard Medical School,Children's Hospital

Hunnewell 4, 300 Longwood Ave, Boston, MA 02115

Running Title: Quantitative MRI of Brain Development in Newborns

This work was supported by grants from the Swiss National Foundation, the Reynolds-Rich-Smith Foundation, and the Charles A. Janeway Scholarship Fund in Child Health Research.

ABSTRACT

Definition in the living premature infant of the anatomical and temporal characteristics of development of critical brain structures is crucial for insight into the time of greatest vulnerability of such brain structures.

We utilized 3D Magnetic Resonance Imaging (3D-MRI) and image processing algorithms to quantitate total brain volume and total volumes of cerebral gray matter (GM), unmyelinated white matter (WM),

myelinated WM and cerebrospinal fluid (CSF) in 78 premature and mature newborns (postconceptional ages: 29 to 41 weeks).

Total brain tissue volume was shown to increase linearly at a rate of 22cc per week. Total GM showed a linear increase in relative intracranial volume of approximately 1.4% or 15cc in absolute volume per week. The pronounced increase in total GM reflected primarily a four-fold increase in cortical GM. Unmyelinated WM was found to be the most prominent brain tissue class in the preterm infant below 36 weeks. Although minimal myelinated WM was present in the preterm infant at 29 weeks, between 35 and 41 weeks an abrupt five-fold increase in absolute volume of myelinated WM was documented. Extracerebral and intraventricular CSF were readily quantitated by this technique and were found to change minimally.

The application of 3D-MRI and tissue segmentation to the study of human infant brain from 29 to 41 weeks postconceptional age has provided new insights into cerebral cortical development and myelination and has for the first time provided means of quantitative assessment *in vivo* of early human brain development.

Key words: brain, development, magnetic resonance imaging, image processing, newborn.

INTRODUCTION

Subsequent neurological disability in infants born prematurely and in term infants who experience perinatal hypoxic-ischemic injury is common and serious [1]. In part, the propensity for such injury may relate to a particular vulnerability of actively developing cerebral gray matter and white matter in the last trimester of human gestation. The anatomical characteristics of these developmental processes have been documented in studies of postmortem human brain [1-7] . Indeed, the occurrence of these processes at this maturational time period may render the brain subjected to ischemia or related insults more vulnerable not only to injury but also to subsequent impairment of gray matter and white matter development. Thus, delineation in the living infant of the anatomical and temporal characteristics of these developmental processes would be of great importance in understanding such maturation-dependent vulnerabilities. Quantitative, volumetric measurements of cerebral gray matter and white matter development, including particularly myelination, in the living premature and term infant would be required to delineate these anatomical and temporal characteristics.

In this prospective study we capitalized on recent advances in magnetic resonance (MR) data acquisition and post-acquisition processing techniques to determine quantitatively in the living human premature and term infant developmental changes in total brain volume and in the total volumes of cerebral gray matter (GM), unmyelinated white matter (WM), myelinated WM and cerebrospinal fluid (CSF). The results delineate in the living infant, for the first time, striking progression of cerebral cortical GM development and of myelination over the critical period of 29 to 41 weeks post conception.

METHODS

Subjects

100 preterm and fullterm infants, gestational age at birth of 28-40 weeks, appropriate weight for gestational age, free of significant medical problems (Table 1) were studied prospectively by MRI within the first 2 weeks of life (postconceptional age at examination: 29-41 weeks) between September

1994 and September 1996. The study was approved by the human subject research committee. No sedation was necessary for the MR studies. The infants were positioned in a vacuum fixation-pillow and monitored by electrocardiography and pulse-oximetry (MR-Equipment Corp, Bay Shore, NY). A neonatologist remained with the infant in the scanner room. Excluded from the final analysis were 22 infants: 13 because of movement artifacts on the MRI, and 9 for unsuspected cerebral pathology noted on the study MRI. Single (35) and multiple gestation infants (43) were analyzed separately.

Image Acquisition

MRI scanning was performed with a 1.5-Tesla General Electric Signa System (GE-Medical Systems Milwaukee). For the acquisition of the primary MR data two different imaging modes were applied, i.e., a three dimensional Fourier Transform spoiled gradient recalled (SPGR) sequence (1.5mm coronal slices, flip angle 45o, repetition time 35ms, echotime 5ms, field of view 18cm, matrix 256x256) and a double-echo {proton density (PD) and T2-weighted} -spin echo sequence (DE) (3mm axial slices, repetition time 3000ms, echo times 36 and 162ms, field of view 18 cm, matrix 256x256, interleaved acquisition). The voxel (volume of pixel) dimensions for the SPGR acquisition were 0.7x0.7x1.5mm and for the spin-echo acquisition 0.7x0.7x3mm. A neuroradiologist evaluated the MRI scans and those showing brain pathology (e.g., intraventricular hemorrhage, periventricular leukomalacia) were excluded from the analysis (9 scans).

Image Processing

Post-acquisition processing was carried out on workstations (Sun Microsystems, Mountain View, California) with newly developed software. A sequence of image processing algorithms was used to segment each of the MRI slices into separate tissue classes: cortical GM, subcortical GM, unmyelinated WM, myelinated WM and CSF. These algorithms were designed to reduce imaging system noise, identify a linear transformation to align the DE spin-echo images with the SPGR images to form a three channel data set, resample the DE spin-echo images according to this transform, classify tissue types on the basis of MR intensity in the three channels and identify tissue class surfaces for 3D visualization. These steps are described briefly as follows:

- Anisotropic diffusion filtering was used to smooth noise without blurring fine details [8].
- The DE spin echo images contain important tissue contrasts, but are acquired with larger voxel size than the SPGR data. A linear reformatation and registration that aligned the DE spin echo images with the SPGR images was computed with an algorithm described by Wells et al.[9].
- As a next step, a k-nearest-neighbor (k-NN) classification was carried out.

This analysis is a supervised nonparametric mulitspectral classification algorithm which identifies tissue classes in the data set by comparison to a set of prototype tissue values selected by an expert operator, knowledgable in both developmental neuronanatomy and pediatric MR-imaging. In this report this step was performed by the first author. Each voxel of the data set is classified by comparing its MRI intensity (in all three channels) with that of the prototypes. Training prototypes in three channels were selected for the following tissue classes: background, skin, CSF, cortical GM, subcortical GM, unmyelinated WM and myelinated WM. Myelinated WM in the newborn MRI has a different signal intensity than unmyelinated WM (see Results). The class that appears most frequently among the k-closest prototypes is chosen as the class of the voxel [10, 11]. A k-value of 5, empirically determined to be optimal, was

applied to compute the classification of every voxel in the datat set. A sample of one automatically segmented slice is given in Figure 1C . A final summing of voxels for each tissue class was performed to compute absolute volumes. Total GM volume was calculated by summing the volumes of cortical and subcortical GM. Relative volumes of the different tissues are reported as percentage of total intracranial volume.

The classification algorithm used has higher accuracy and stability for MRI data than other statistical classifiers [12]. Classification error rates and reproducibility have been calculated and are approximately 5% for number of neighbors k >3 [13].

Surface models were obtained by triangulation of the classified volume with the marching cubes algorithm[14]. 3D-visualization of distribution of brain tissues in vivo was achieved by 3D-rendering of the segmentation data.

Statistical Analysis

To test the relationship between specific brain tissue volumes (total GM, cortical and subcortical GM, unmyelinated and myelinated WM, CSF) and postconcpetional age, a linear regression model was used. For the relationships between unmyelinated WM, myelinated WM, and postconceptional age, a logarithmic transform of the data was used before fitting the linear model.

Coefficients of determination (r2) are given with p-values to accept or reject significant correlation of brain tissue volumes and postconceptional age. Differences of single vs. multiple gestation infants and female vs. male infants were tested in the multiple regression model using the interaction term. Within the interaction term we assessed differences in the y-intercept (a) as well as in the slope (b)[15].

RESULTS

Quantitative volumetric analysis of brain development was carried out in the 78 infants (35 of single gestation and 43 of multiple gestation). The maturational time period of the study was 29 to 41 weeks post conception because the infants, whose gestational age ranged from 28 to 40 weeks, were studied in the first two postnatal weeks. Quantitative determinations of total brain volume and individual volumes of GM (cortical and subcortical), WM (unmyelinated and myelinated) and CSF (extracerebral and intraventricular) were carried out, as described next.

Total Brain Volume

Total brain tissue volume, including cerebral hemispheres, cerebellum and brainstem but excluding CSF, showed a significant linear increase from approximately 150 cc at 29 weeks postconceptional age to approximately 400cc at fullterm. The rate of increase was 22cc per week (Figure 2). There was no difference in total brain volumes between single and multiple gestation infants (p-value for y-intercept =0.076; p-value for slope =0.183). Although the rate of increase of total brain volumes was similar for female and male infants (p-value for slope =0.157), female infants of identical postconceptional age as male infants had significantly smaller total brain volumes (female brain volume=-453.5+20.6 x postconceptional age [i.e., 30wks:165cc], male brain volume=-430.5+20.6 x postconceptional age [i.e., 30wks:188cc] (p-value for the y-intercept =0.02).

Brain Tissue Volumes

The sequential changes in specific brain tissues, i.e., total GM, cortical GM, unmyelinated WM, myelinated WM and CSF are shown in Figures 3, 4, 7, 8, 10 for single gestation infants only. Values are provided as percentage of total intracranial volume and as absolute values (cc).

Gray Matter Volumes: Total, Cortical and Subcortical

Total GM, which includes cortical and subcortical GM as differentiated by automatic segmentation, showed a linear increase in relative intracranial volume of approximately 1.4% per week (Figure 3A). At 30 weeks postconceptional age GM represented approximately 35% of total brain volume; GM volume was 60cc in a total brain volume of approximately 160cc (Figure 3B). At term, GM represented 50% of total brain volume, i.e., 200cc in a total brain volume of approximately 400cc. The increase in absolute values of total GM volume from 30 to 40 weeks thus was approximately three-fold.

The pronounced increase in total GM reflected primarily an increase in cortical GM, as shown in Figures 4A and B. From 29 weeks to 41 weeks post conception, the relative intracranial volume of cortical GM increased from approximately 20% to approximately 40% (Figure 4A). The increase in absolute values of cortical GM volume was fully four-fold, i.e., from 40cc at 30 weeks to 160cc at 40 weeks (Figure 4B). The marked increase in cerebral gyration and therefore cortical GM is shown clearly by the MR images (Figure 5) and the 3D rendering of the cerebral surface (Figure 6). In contrast to the marked changes in cortical GM, subcortical GM, including principally basal ganglia and thalami, showed no significant volume changes during the observed period of brain development (data not shown).

White Matter Volumes: Unmyelinated and Myelinated

Unmyelinated WM was found to be the most prominent brain tissue class in the preterm infant below 36 weeks postconceptional age and at 29-30 weeks accounted for approximately 48% of total intracranial volume (Figure 7A) and 65% of total brain volume (compare Figure 7B and Figure 2). At 36 weeks the relative intracranial volumes of total GM and of unmyelinated WM were similar (compare Figures 3A and 7A). Subsequently the relative volume of GM exceeded that of unmyelinated WM. A clear decrease in relative volume of unmyelinated WM became apparent near term (Figure 7A), despite a slight increase in absolute values of unmyelinated WM during the same period (Figure 7B). The slight increase in absolute values of unmyelinated WM despite its declining relative intracranial proportion resulted because of the increase in total brain volume (Figure 2).

Changes in both the relative and absolute volumes of myelinated WM were dramatic. Thus, the relative volume of myelinated WM began to increase at around 35-36 weeks (Figure 8A). Between 29 and 34 weeks the relative intracranial volume of myelinated WM was 1-2% (Figure 8A), and the corresponding absolute value was 3-4 cc (Figure 8B). A rapid increase occurred after 36 weeks such that at 41 weeks the relative intracranial volume of myelinated WM had increased markedly to 5% (Figure 8A) and the corresponding absolute volume had increased to approximately 20cc (Figure 8B). Thus, the increase in absolute volume of myelinated WM from 29 to 41 weeks was approximately five-fold. Changes in myelinated WM are shown well by the MR images (Figure 9).

Cerebrospinal Fluid Volume (CSF)

The relative intracranial volume of total CSF, which comprises extracerebral (including sulcal) and ventricular CSF, decreased slightly from 29 to 41 weeks, i.e., total CSF accounted for approximately 10-15% of intracranial volume at 29-31 weeks and 8-10% at term (Figure 10A). With total brain growth absolute values of CSF showed a slight increase between 29 and 41 weeks (Figure 10B). At term, intraventricular CSF volume accounted for 2-3% of intracranial volume (data not shown) and therefore approximately 25% of total CSF volume.

Multiple Gestation Infants

As noted earlier, there was no difference in total brain volumes between single and multiple gestation infants. However, in the multiple gestation infants the relative intracranial volume of total GM did not increase (data not shown), unlike the significant increase defined in singletons (Figure 3A). Moreover, although in the multiple gestation infants the relative volume of cortical GM did increase slightly, at a rate of 0.6% per week (Figure

11), this increase was significantly lower than the 1.5% per week increase defined in single gestation infants (p-value for slope difference =0.024). Consistent with this result, comparison of single vs. multiple gestation infants for the developmental increase in absolute values of cortical GM in two maturational groups (group 1, postconceptional age=29-33 weeks, and group 2, postconceptional age=33-37 weeks) showed a significant difference in absolute cortical GM volumes only in the more mature group (Table 2).

Because we did not have the opportunity to study any multiple gestation infants after 37 weeks postconceptional age, it was difficult to compare such infants to singletons concerning changes in relative volumes of unmyelinated WM and myelinated WM. As noted earlier, the decrease in relative volume of unmyelinated WM and the sharp increase in relative volume of myelinated WM occurred in the last weeks prior to term (see Figures 7 and 8). Thus, perhaps not surprisingly, there was no significant change in cerebral unmyelinated WM or myelinated WM in the multiple gestation infants over the maturational range studied, i.e., 30 to 37 weeks (data not shown). Both relative and absolute CSF volumes also were not different between single and multiple gestation infants (data not shown).

DISCUSSION

Post-acquisition MR processing techniques, using tissue segmentation methods with 3D-renderings, have been developed and applied previously in adults and infants to improve volume visualization and to make possible absolute quantification [16-25]. Studies to date have focused principally either on the adult and older infant, at timepoints when major brain growth and structural development are largely completed, or in a small number of newborns without specific quantitation of cortical GM or myelinated vs. unmyelinated WM [23].

This report has utilized quantitative, volumetric MRI techniques in 78 consecutively studied infants to delineate anatomical and temporal characteristics of brain development in a time period of extreme relevance to brain injury in the premature and term infant, i.e., 29 to 41 weeks of postconceptional age. Quantitative assessment of cerebral cortical GM development and of myelination thus has been achieved for the first time by an in vivo technique. The marked changes in both cerebral GM and WM development provide important insights into normal human brain development during this crucial

period. The findings also have potentially important implications for the maturation-dependent vulnerability of premature and term infant brain both to specific types of ischemic injury and to subsequently altered brain development. Moreover, the observations suggest great promise for future clinical applications of this technique.

Total Brain Volume

Using 3D-MRI and tissue segmentation we were able to measure noninvasively total brain tissue volume exclusive of CSF and to define a 2.7-fold increase from 29 to 41 weeks of postconceptional age. This increase was similar in male and female infants, although at a given postconceptional age male infants had slightly larger brain volumes than did female infants. The latter difference is similar to that in body weight and length in male vs. female infants and thus defines an early difference in brain size, which continues into adulthood [22, 23].

The ability to determine total brain volume will be important clinically in the assessment of overall brain growth. Currently determination of head growth by measurement of head circumference is utilized to monitor brain growth, since abnormalities of brain growth have prognostic implications concerning neurological development [26]. However, interpretation of measurements of head growth, especially in premature infants, is rendered difficult by the inability to differentiate the relative importance of total brain tissue volume vs. CSF volume in determining such growth. The quantitative MRI technique described in this report makes this differentiation highly effectively.

Gray Matter Volumes

The principal determinant of the increase in total brain volume from 29 to 41 weeks postconceptional age was an increase in GM volume. Indeed, the proportion of brain volume represented by GM volume increased from approximately 35 to 50% from 29 weeks to term, and the absolute values for GM volume increased about three-fold during this period.

The marked increase in total GM volume was related to a sharp increase in cortical GM volume rather than in subcortical GM volume. An approximately four-fold increase in absolute cortical GM volume occurred from 30 to 40 weeks. The basis for the increase in cortical GM volume almost certainly relates primarily to neuronal differentiation rather than to an increase in numbers of neurons. Indeed, in the human brain neuronal migration to cerebral cortex is complete by approximately 20-24 weeks of gestation [27]. However, the elaboration of dendritic and axonal branching is a prominent feature of human cerebral cortical development during the time period of our study [1]. Indeed, the changes in surface area that occur as a consequence of this neuronal differentiation result in the stresses that lead to gyral development [28-31]. The development of secondary and tertiary gyri is dramatic in human brain in the last trimester of gestation [2, 32], as illustrated clearly by our 3D MRI images (see Figure 6).

The ability to determine cortical GM volume will be important clinically in detecting abnormalities of cerebral cortical development that result subsequent to destructive insults or occur as a consequence of a primary dysgenetic disturbance. Such quantitative assessment of gyral development is not possible by conventional brain imaging modalities.

White Matter Volumes

Prior to approximately 36 weeks postconceptional age, WM is quantitatively the most prominent brain

tissue class. Unmyelinated WM accounts for approximately 98% of total WM volume during this period. Prior to 36 weeks myelinated WM is the least abundant brain tissue class and accounts for only approximately 3-4cc of total WM volume.

After 36 weeks postconceptional age a dramatic increase in myelinated WM volume becomes apparent. Indeed, from 29 weeks to term the absolute values of myelinated WM increase approximately five-fold, and most of this increase occurs after 36 weeks. This conclusion, of course, relates to MR-visible myelin. Current data indicate that the MR signal is generated by myelin lipid precursors (cholesterol, glycolipids) [33]. Studies of autopsied human brain also suggest rapid evolution of human cerebral myelination at this developmental time [4, 34, 35].

The clinical importance of these observations is at least two-fold. First, the dramatic increase in myelinated WM volume suggests a period of rapid development and thereby a time of vulnerability of WM to injurious insults. Indeed, injury to WM caused by ischemia is the most common form of brain injury encountered in the human premature infant [1, 36, 37].Second, the effects of a variety of other postnatal insults common in premature infants (including abnormalities of nutrition, thyroid function, metabolic homeostasis, etc.) on subsequent myelination now can be determined by this quantitative assessment of myelinated WM development. Considerable experimental data suggest that such insults may lead to impairment of subsequent myelination [38-40] but studies in human infants are lacking. This lack relates primarily to the difficulty of quantitating myelination by conventional brain imaging techniques, a difficulty now surmounted by the MR approach utilized in this study.

CSF Volumes

Although there were no clear developmental changes in CSF volume from 29 to 41 weeks, the ability to quantitate separately both ventricular and extracerebral CSF volumes has important clinical implications. Thus, a common complication of prematurity is the development of impaired CSF dynamics, i.e., hydrocephalus following intraventricular hemorrhage, the latter occurring in approximately 25% of infants of <1500 gm birthweight or approximately 32 weeks of gestation [1]. Quantitative definitions of the progression of this hydrocephalic state and the response of the hydrocephalus to various therapies are not accomplished readily by available brain imaging techniques. Quantitation of CSF volumes, as accomplished in this study, would be a very important adjunct in this clinical setting.

Multiple Gestation Infants

Although total brain volume did not differ between multiple gestation infants and singletons, lower values for cortical GM volume were apparent in multiple gestation infants at 34-37 weeks (see Table 2). Thus, at this postconceptional age, absolute values for cortical GM in the multiple gestation infants were approximately 80% of the values in singletons. Interestingly, no difference in cortical GM volume was apparent between multiple gestation infants and singletons at 29-33 weeks. The observations raise the possibility that cortical GM development is delayed in multiple gestation infants born after 33 weeks of gestation. Such a delay could relate to the occurrence of placental insufficiency later in multiple pregnancies. A neuropathological correlate of our finding of lower cortical GM volume may be the finding of a delay of 2-3 weeks in the appearance of convolutional markings in twin gestations [2]. A possible clinical correlate for the delay in cortical GM development may be the finding of later cognitive differences between singletons and twin infants [41, 42].

CONCLUSIONS

The application of 3D-MRI and tissue segmentation to the study of human infant brain from 29 to 41 weeks postconceptional age has provided new insights into cerebral cortical development and myelination. The technique allows non-observer-biased quantitation of brain tissues in vivo in a manner not possible previously with conventional imaging techniques. The findings have defined phases of rapid developmental progression and, by implication, potential critical periods of vulnerability to endogenous and exogenous factors. Such factors include premature birth, hypoxia-ischemia, intracranial hemorrhage, infection, undernutrition, administration of drugs and hormones, sensory deprivation and excess, etc. Future studies of infants subjected to such insults should allow delineation of their impact on specific aspects of brain development.

ACKNOWLEDGEMENT

The authors are thankful to William Wells, Ph.D., and Tina Kapur, Ph.D., for the program source for registration and their help in the implementation and improvement of the image processing steps, to the MR-team for their technical assistance, and to the parents of the patients for consent to participation in this study.

Respiratory distress syndrome requiring mechanical ventilation >24h
Perinatal acidosis or asphyxia
Intraventricular hemorrhage
Seizures
Abnormal neurological exam
Sepsis
Intrauterine growth retardation
Malformations
Hypoglycemia

Table 1: Exclusion Criteria for Study Group

	Gray Matter Volume (ml)		
Postconceptional age (weeks)	Singletons (n=35) (mean±SD)	Multiples (n=43) (mean±SD)	p value
29-33	57.1±16.5	58.2±6.9	0.843
34-37	108.2±21.4	85.4±23.2	0.006

Table 2: Absolute Cortical Gray Matter Volumes (cc) in Single and Multiple Gestation Infants

FIGURES

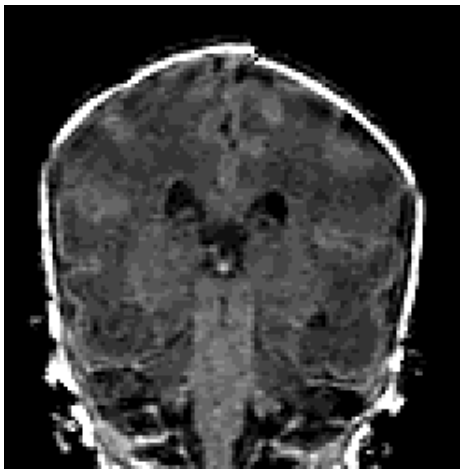

Figure 1A: T1-weighted MR-image (SPGR), coronal plane in a preterm infant (31 wks)

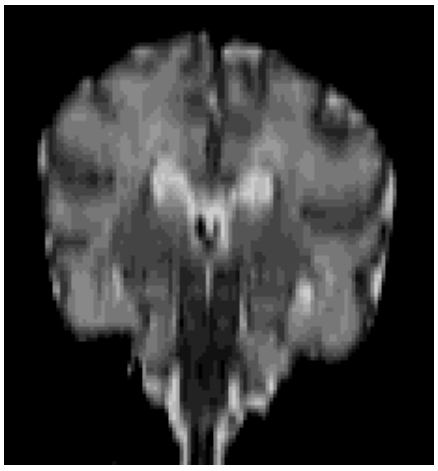

Figure 1B: T2-weighted MR-image reformatted from axial to coronal plane and registered with SPGR image.

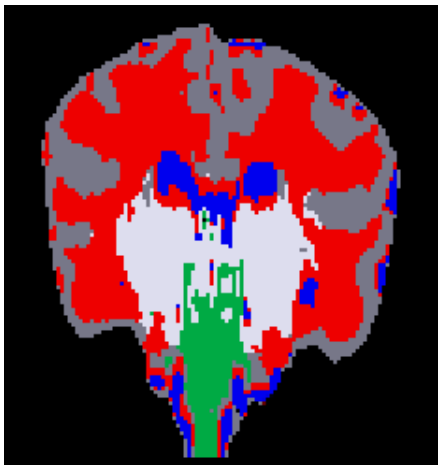

Figure 1C: Final segmented image depicting cortical GM in gray, unmyelinated WM in red, CSF in blue, myelinated WM in green and subcortical GM (basal ganglia) in white.

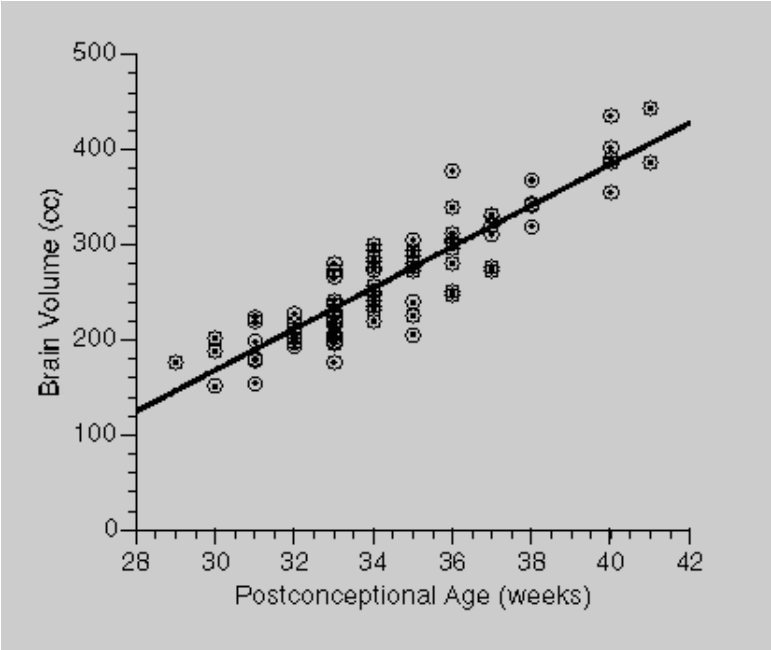

Figure 2: Scatterplot showing total brain volume (cc) (intracranial volume - CSF volume) in all infants. The linear regression model fits the data with a coefficient-of-determination r2=0.8 and p<0.001. [Brain Volume=21.6 x postconceptional age(weeks) - 481.6]

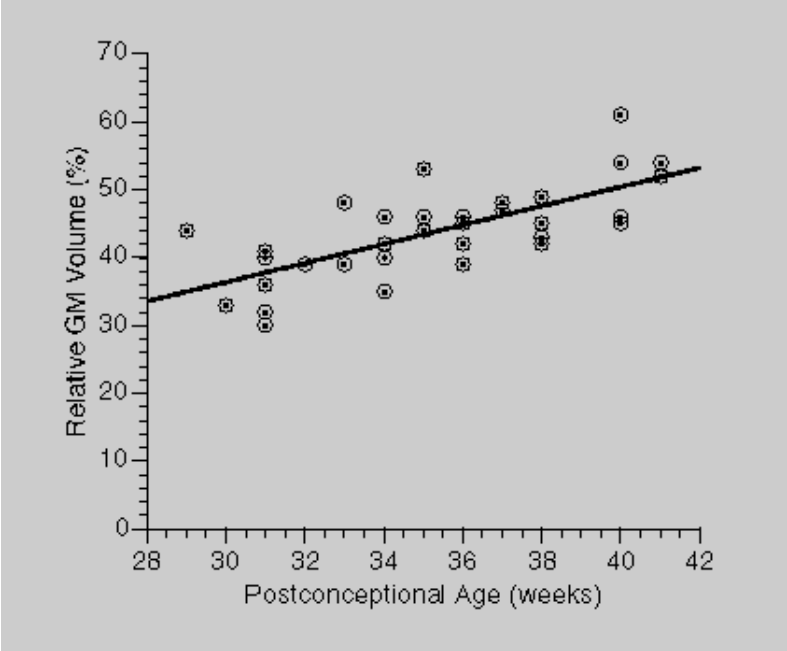

Figure 3A: The scatterplot shows the relative volume of total brain GM as a percentage of intracranial volume in single gestation preterm and fullterm infants (n=35). The linear regression model fits the data with a coefficient-of-determination r2=0.5 and p<0.001. [GM=1.4 x postconceptional age(weeks) -5.73].

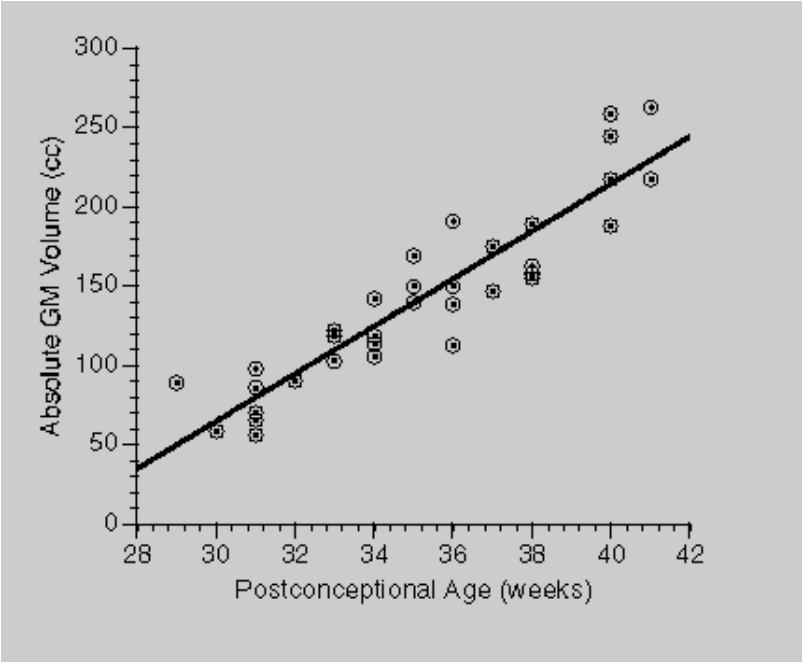

Figure 3B: The scatterplot shows the absolute volume of brain GM in single gestation preterm and fullterm infants (n=35). The linear regression model its the data with a coefficient-of-determination r2=0.8 and p<0.001. [GM=14.9 x postconceptional age(weeks) - 382.7].

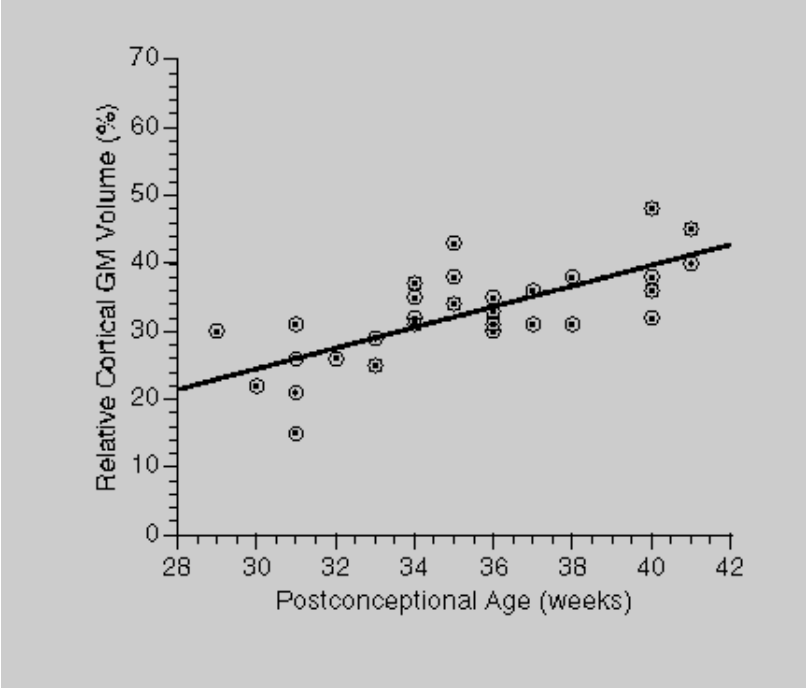

Figure 4A: The scatterplot shows the relative volume of cortical GM as a percentage of intracranial volume in single gestation preterm and fullterm infants (n=35). The linear regression model fits the data with a coefficient-of-determination r2=0.5 and p<0.001. [Cortical GM=1.5 x postconceptional age(weeks) - 2.13]

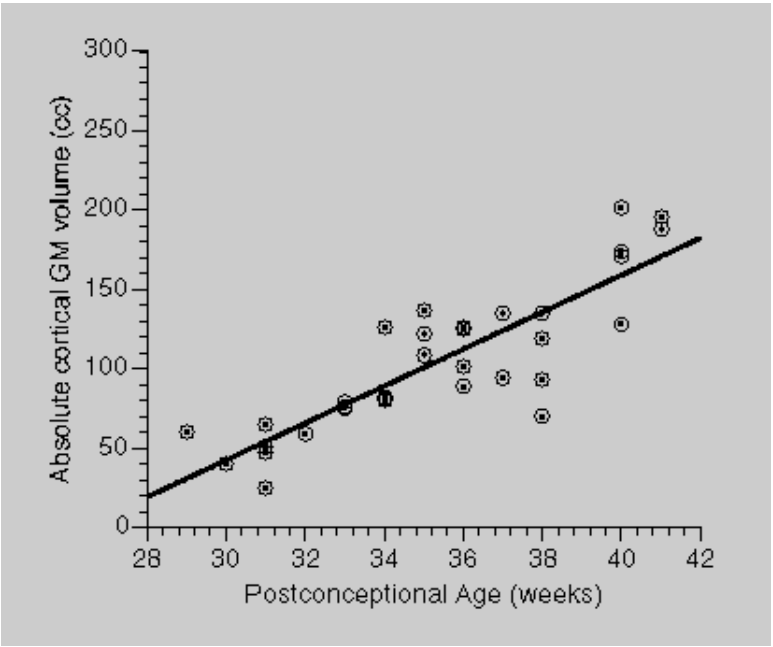

Figure 4B: The scatterplot shows the absolute volume of brain cortical GM in single gestation preterm and fullterm infants (n=35). The linear regression fits the data with a coefficient-of-determination r2=0.7 and p<0.001. [GM=11.6 x postconseptional age(weeks) - 307.7].

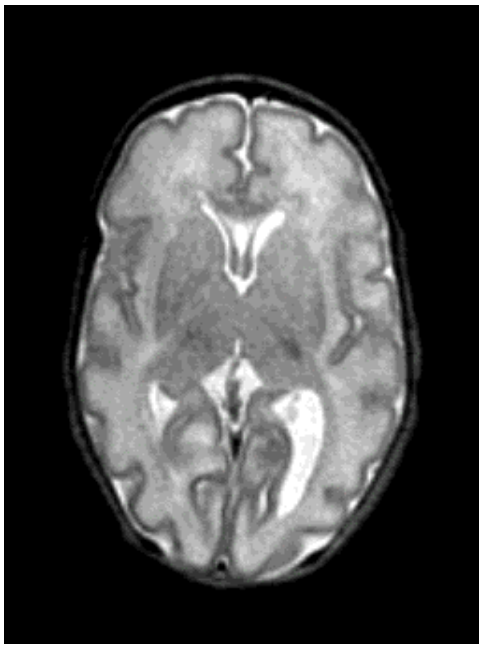

Figure 5A: Axial T2 spin-echo MR (3000/160) image in a preterm infant at 31weeks postconceptional age. The cerebral cortex is relatively hypotense and the cerebral white matter is relatively hyperintense. The gyral pattern is relatively simple.

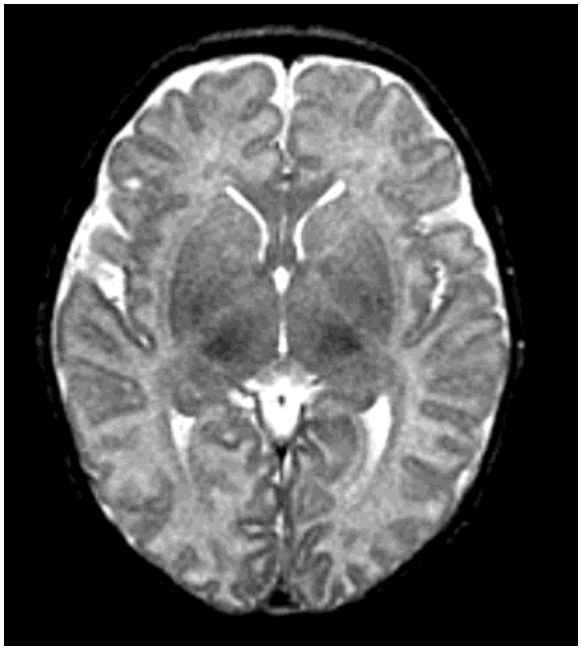

Figure 5B: Axial T2 spin-echo MR (3000/160) image in a fullterm infant at 40weeks postconcpetional age. Increased gyration is striking compared to A.

A: 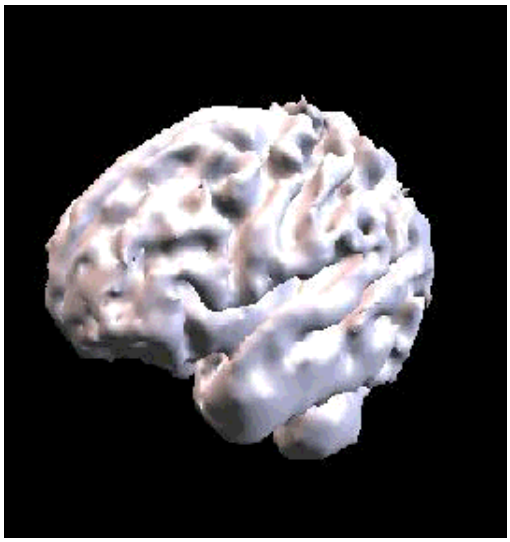 B: 

Figure6: 3D brain model of a preterm infant (31weeks) (A) and a fullterm infant (40 weeks) (B): 3D rendering after tissue segmentation using post-processing techniques. The marked increase of gyral pattern in the fullterm infant compared to the preterm infant is well-shown.

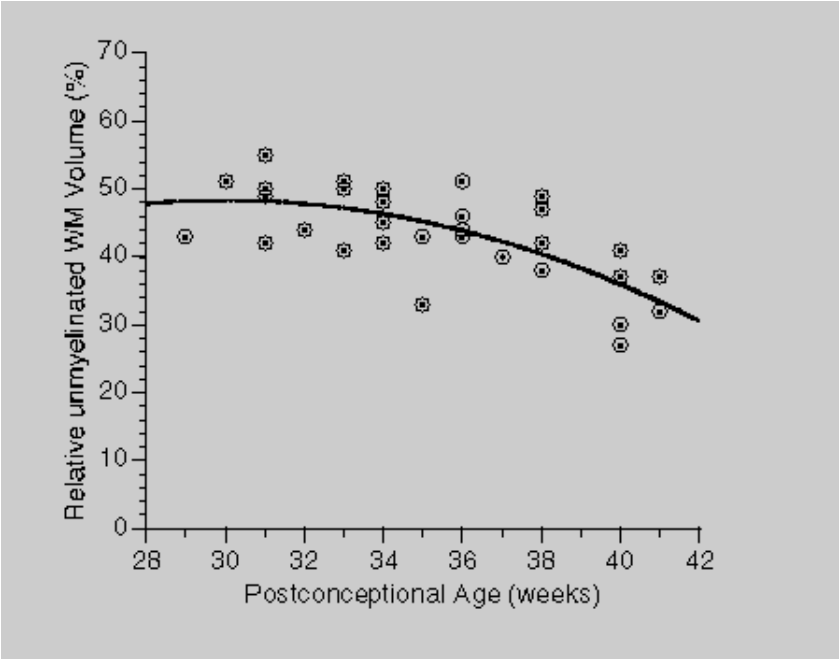

Figure 7A: The scatterplot shows the relative volume of unmyelinated WM as a percentage of intracranial volume in single gestation preterm and fullterm infants (n=35). The polynomial function fits the data [Unmyelinated WM= -0.12 x postconceptional age(weeks) + 7.4 x postconceptional age(weeks) - 6.29]. Log unmyelinated WM was used for the calculation of the linear regression model with $r2=0.4$ and $p<0.001$.

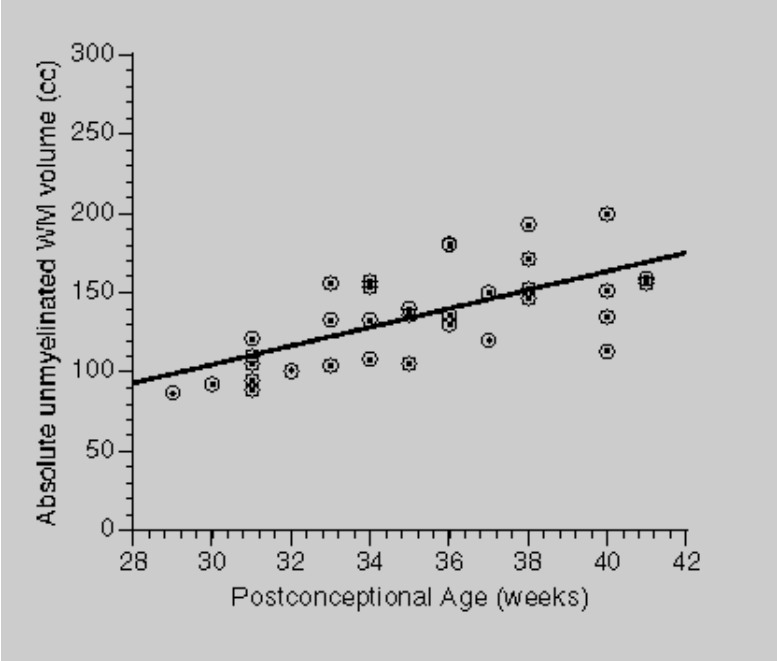

Figure 7B: The scatterplot shows the absolute volume of unmyelinated WM in single gestation preterm and fullterm infants (n=35). The linear regression fits the data with a coefficient-of-determination r2=0.4 and p<0.001. [Unmyelinated WM = 5.8 x postconceptional age(weeks) - 71.6].

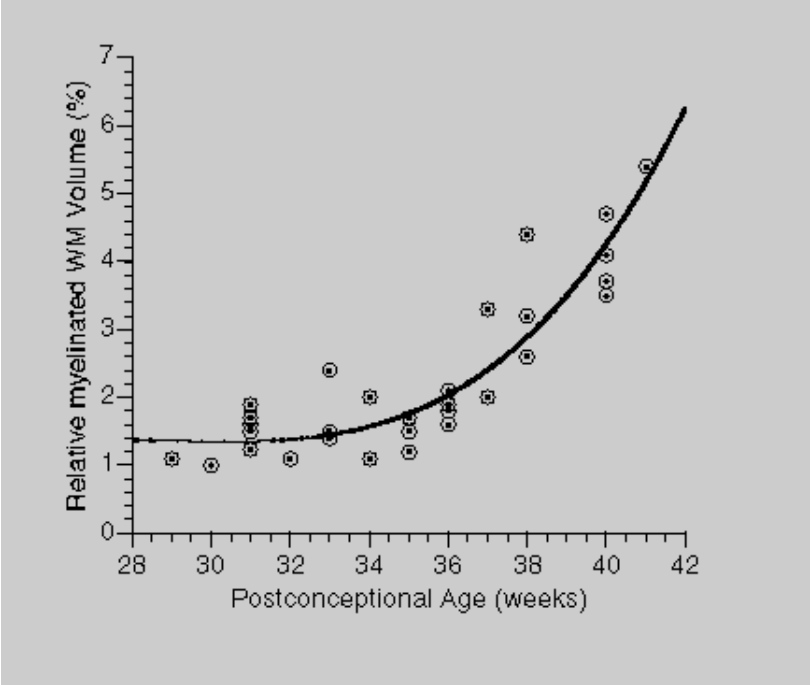

Figure 8A: The scatterplot shows the relative volume of myelinated WM as a percentage of intracranial volume in single gestation preterm and fullterm infants (n=35). The polynomial function fits the data [Myelinated WM=0.002 x postconceptional age(weeks) - 0.22 x postconceptional age(weeks) + 6.3 x postconceptional age(weeks) - 60.2]. A logarthmic transform of myelinated WM was used for the

calculation of the linear regression model with r2=0.6, and p<0.001.

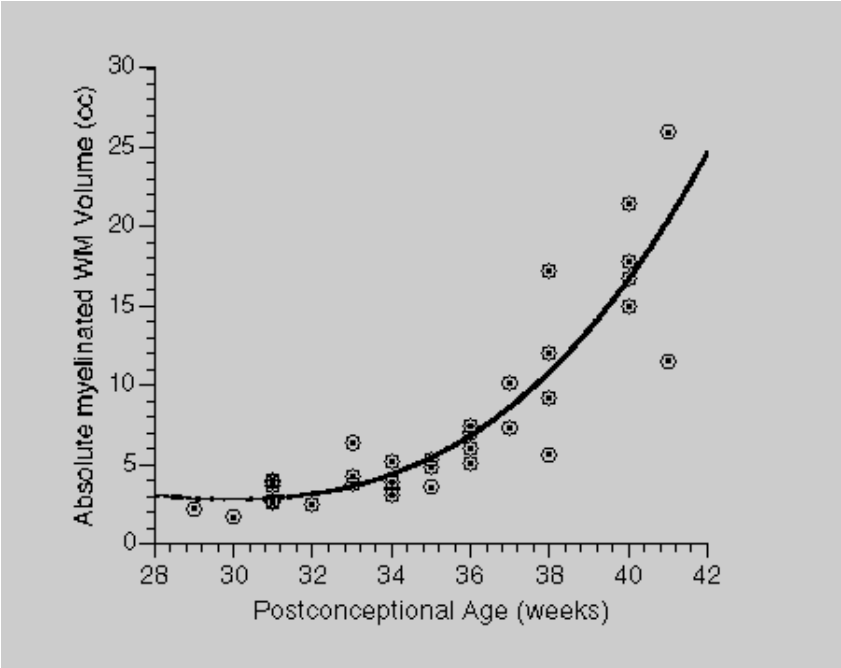

Figure 8B: The scatterplot shows the absolute volume of myelinated WM in single gestation preterm and fullterm infants (n=35). The polynomial function fits the data [Myelinated WM= 0.006 x postconceptional age(weeks) - 0.5 x postconceptional age(weeks) +13.5 x postconceptional age(weeks) -111.3]. Log [Myelinated WM] was used for the calculation of the linear regression model with r2=0.8 and p<0.001.

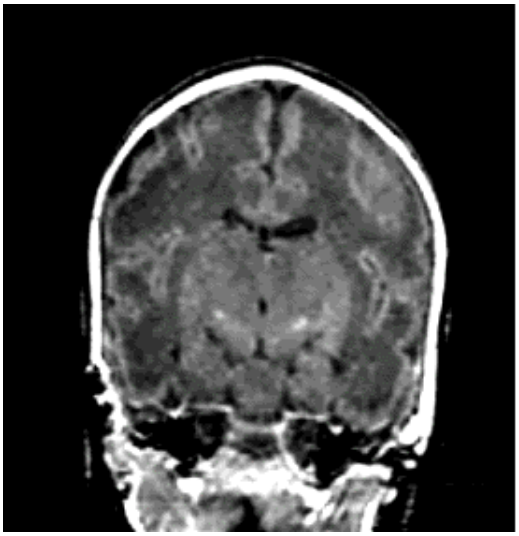

Figure 9A: Coronal SPGR (35/5/45o) MR image obtained in a preterm infant at 31 weeks postconceptional age shows minimal amount of myelinated WM (arrows) in the parathalamic region of the internal capsule.

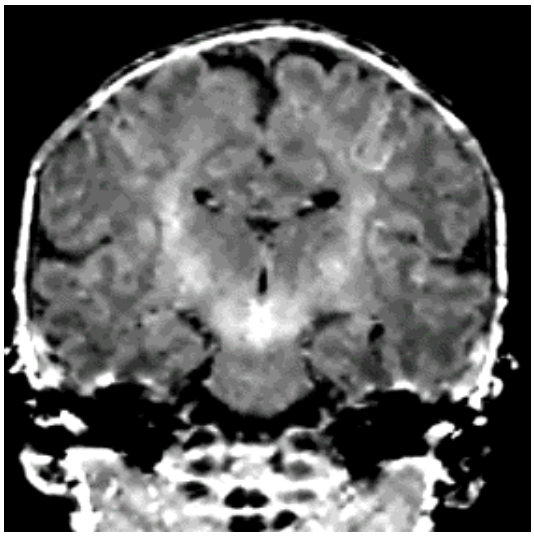

Figure 9B: Coronal SPGR (35/5/45o) MR image obtained in a fullterm infant at 40 weeks postconceptional age shows myelinated WM in internal capsule and central white matter of corona radiata (arrows).

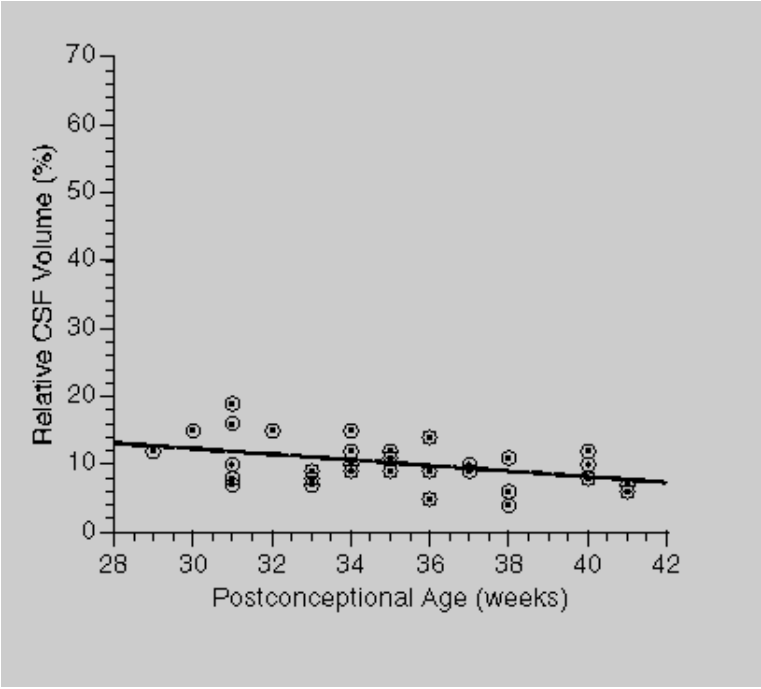

Figure 10A: The scatterplot shows the relative volume of extracerebral and intraventricular CSF as a percentage of the intracranial volume in single gestation preterm and fullterm infants (n=35). The linear regression model fits the data with a coefficient-of-determination r2=0.17 and p=0.057. [CSF=-0.4 x postconceptional age(weeks) + 2.46].

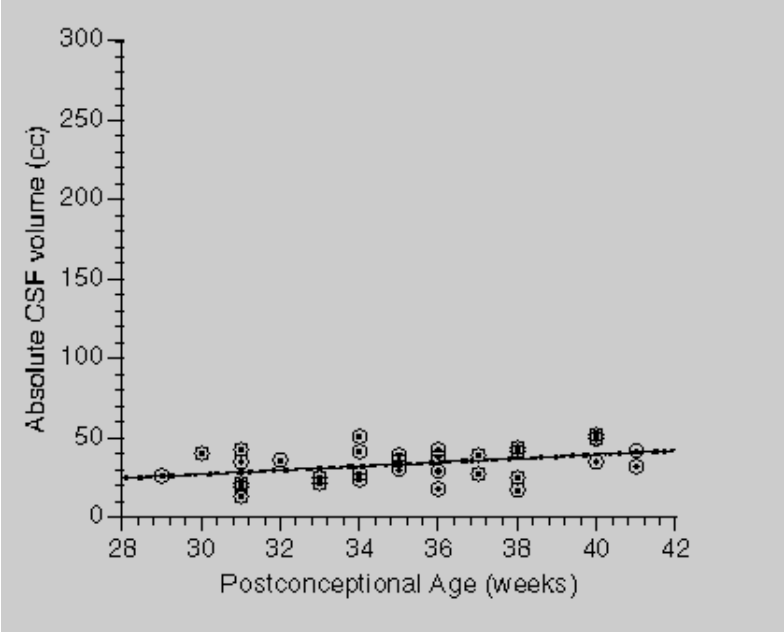

Figure 10B: The scatterplot shows the absolute volume of extracerebral and intraventricular CSF in single gestation preterm and fullterm infants (n=35). The linear regression model fits the data with a coefficient-of-determination r2=0.1, and $p<0.05$. [CSF=1.2 x postconceptional age(weeks) - 10.2].

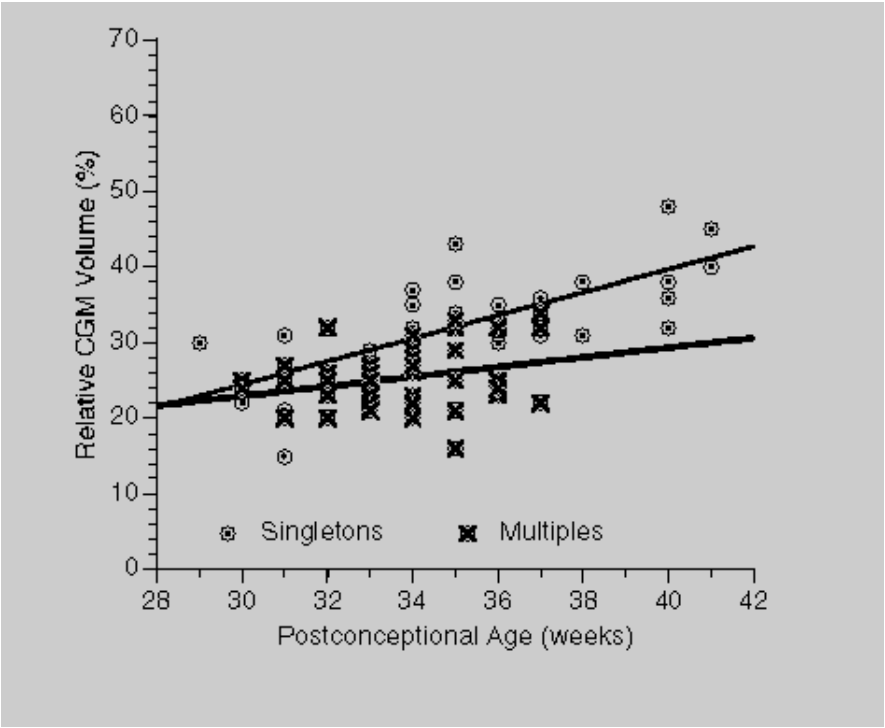

Figure 11: The scatterplots show the relative volumes of the cortical GM in all singleton preterm and fullterm infants and in infants from multiple gestation, in separate scatterplots (n=78). Linear regression models were fitted for both groups. The increase of cortical GM volume in singletons is given by the regression equation coefficient b S=1.5% per week. The increase of cortical GM volume in the multiple

gestation infants is given by b M=0.6%. per week. This difference in slope was significant using multiple regression analysis (p-value for slope difference p=0.024).

REFERENCES

1. Volpe JJ. *Neurology of the Newborn*. 3rd Edition. WB Saunders, Philadelphia, 1995.

2. Chi JG, Dooling EC, Gilles FH. Gyral development of the human brain. Ann Neurol 1977; 1: 86-93.

3. Dobbing J., Sands J. Quantitative growth and development of human brain. Arch Dis Child 1973; 48: 757-67.

4. Gilles FH. Myelination in the neonatal brain. Human Pathology 1976; 7: 244-248.

5. Leviton A, Gilles FH. Morphologic abnormalities in human infant cerebral white matter related to gestational and postnatal age. Pediatr Res 1974; 8: 718-720.

6. Marin-Padilla M. Prenatal and early postnatal ontogenesis of the human motor cortex: A Golgi study. I. The sequential development of the cortical layers. Brain Res 1970; 23: 167-183.

7. Evrard P, Gressens P, Volpe JJ. New concepts to understand the neurological consequences of subcortical lesions in the premature brain. Biol Neonate 1992; 61:1-3.

8. Gerig G, Kübler O, Kikinis R. Nonlinear anisotropic filtering of MRI data. IEEE TMI 1992; 11: 221-232.

9. Wells W, ed. Multimodal registration by maximization of mutual information. Medical Image Analysis, Vol. 1. 1996, Oxford College Press.

10. Warfield S, Dengler J, Zaers J, Guttman RG, Wells WM, Ettinger GJ, Hiller J, Kikinis R. Automatic identification of grey matter structures from MRI to improve the segmentation of white matter lesions. J Image Guid Surg 1996; 1: 326-338.

11. Friedman JH, Baskett F, Shustek LJ. An algorithm for finding nearest neighbors. IEEE Transactions on Computers 1975; C-24: 1000-1006.

12. Clarke LP, Velthuizen RP, Phuphanich S, Schellenberg JD, Arrington JA, Sibriger M. Stability of three supervised segmentation techniques. Magn Reson Imag 1993; 11: 95-106.

13. Warfield S. Fast knn classification for multichannel image data. Pattern Recognition Letters 1996; 17: 713-721.

14. Lorenson WE, Cline HE. Marching cubes: a high resolution 3D surface reconstruction algorithm. Comp Graph 1987; 21: 163-169.

15. Pagano M, Gauvreau K. *Principles of Biostatistics*. Edition. Wadsworth Publishing Company, Belmont, CA, 1993; pp 414-422.

16. Caviness VS, Filipek PA, Kennedy DN. Quantitative magnetic resonance imaging and studies of degenerative diseases of the developing human brain. Brain Dev 1992; 14 (suppl): S80-S85.

17. Filipek PA, Kennedy DN, Rademacher J, Caviness VS. MRI-based morphometry:development and applications to normal controls. Ann Neurol 1989; 25: 61-67.

18. Jernigan TL, Tallal P. Late childhood changes in brain morphology observable with MRI. Dev Med Child Neurol 1990; 32: 379-385.

19. Jernigan TL, Trauner DA, Hesselink JR, Tallal PA. Maturation of the human cerebrum observed in vivo during adolescence. Brain 1991; 114: 2037-2949.

20. Andreasen N. C., Harris G., Cizadlo T., Arndt S, O?Leary DS, Swayze V, Flaum M. Techniques for measuring sulcal/gyral patterns in the brain as visualized through magnetic resonance scanning: BRAINPLOT and BRAINMAP. Proc Natl Acad Sci U S A 1994; 91: 93-7.

21. Shenton M. E., Kikinis R., Jolesz F. A., Pollak SD, LeMay M, Wible CG, Hokama H, Martin J, Metcalf D, Coleman M. Abnormalities of the left temporal lobe and thought disorder in schizophrenia. A quantitative magnetic resonance imaging study. N Engl J Med 1992; 327: 604-12.

22. Pfefferbaum A, Mathalon DH, Sullivan EV, Rawles JM, Zipursky RB, Lim KO. A quantitative magnetic resonance imaging study of changes in brain morphology from infancy to late adulthood. Arch Neurol 1994; 51: 874-887.

23. Toft PB, Leth H, Ring PB, Peitersen B, Lou HC, Henriksen D. Volumetric analysis of the normal infant brain and in intrauterine growth retardation. Early Hum Dev 1995; 43: 15-29.

24. Katzman DK, Lambe K, Mikulis DJ, Ridgley N, Goldbloom DS, Zipursky RB. Cerebral gray matter and white matter volume deficits in adolescents girls with anorexia nervosa. J Pediatr 1996; 129: 794-803.

25. Matsumae M, Kikinis R, Morocz IA, Lorenzo AV, Sandor T, Albert MS, Black P, Jolesz FA. Age-related changes in intracranial compartment volumes in normal adults assessed by magnetic resonance imaging. J Neurosurg 1996; 84: 982-991.

26. Hack M, Breslau N, Weissman B, Aram D, Klein N, Borawski E. Effect of very low birth weight and subnormal head size on cognitive abilities at school age. N Engl J Med 1991; 325: 231-237.

27. Rakic P. Limits of neurogenesis in primates. Science 1985; 227: 1054-1056.

28. Turner OA. Growth and development of the cerebral cortical pattern in man. Arch Neurol Psych 1948; 59: 1-12.

29. Richman D, Stewart R, Hutchinson JW. Mechanical model of brain convolutional development. Science 1975; 189: 18.

30. Rakic P. Specification of cerebral cortical areas. Science 1988; 241: 170-176.

31. Kostovic I, Rakic P. Developmental history of the transient subplate zone in visual and somatosensory cortex of the macaque monkey and human brain. J Comp Neurol 1990; 297: 441-470.

32. Dorovini-Zis K, Dolman CL. Gestational development of brain. Arch Pathol Lab Med 1977; 101: 192-195.

33. Barkovich AJ, Gilles L, Evrard P. Formation, maturation,and disorders of white matter. AJNR 1992; 13: 447-461.

34. Kinney HC, Brody BA, Kloman AS, Gilles FH. Sequence of central nervous system myelination in human infancy. II Patterns of myelination in autopsied infants. J Neuropathol Exp Neurol 1988; 47(3): 217-234.

35. Yakovlev PI, Lecours AR. The myelogenetic cycles of regional maturation of the brain. In: Minkowski A, eds. *Regional Development of the Brain in Early Life*. Philadelphia: Davis, FA:1967

36. Volpe JJ. Brain injury in the premature infant-current concepts of pathogenesis and prevention. Biol Neonate 1992; 62: 231-242.

37. Murphy DJ, Squier MV, Hope PL, Sellers S, Johnson A. Clinical associations and time of onset of cerebral white matter damage in very preterm babies. Arch Dis Child 1996; 75: F27-F32.

38. Timiras PS, Nzekwe EU. Thyroid hormones and nervous system development. Biol Neonate 1989; 55: 376-385.

39. Wiggins RC. Myelin development and nutritional insufficiency. Brain Res Rev 1982; 4: 151-175.

40. Royland JE, Konat G, Wiggins RC. Abnormal upregulation of myelin genes underlies the critical period of myelination in undernourished developing rat brain. Brain Res 1993; 607: 113-116.

41. Wilson RS. Twin growth: Initial deficit, recovery, and trends in concordance from birth to nine years. Ann Hum Biol 1979; 6: 205-220.

42. Petterson B, Nelson KB, Watson L, Stanley FJ Twins, triplets and cerebral pasly in births in Western Australia in the 1980s. Br Med J 1993; 307: 1239-1243